water

MDPI

Article

Holocene Hydroclimatic Changes in Northern Peloponnese (Greece) Inferred from the Multiproxy Record of Lake Lousoi

Dionysios Stamatis [1], Alexandros Emmanouilidis [1], Alessia Masi [2], Adam Izdebski [3] and Pavlos Avramidis [1,*]

[1] Department of Geology, University of Patras, 26504 Patras, Greece; sdionyses@gmail.com (D.S.); alex.emman@upatras.gr (A.E.)
[2] Dipartimento di Biologia Ambientale, Sapienza Universita Di Roma, Via Cesare de Lollis, 21, 00185 Rome, Italy; alessia.masi@uniroma1.it
[3] Max Planck Institute for the Science of Human History, Kahlaische Strasse 10, 07745 Jena, Germany; izdebski@shh.mpg.de
* Correspondence: p.avramidis@upatras.gr

Abstract: This research presents the paleoenvironmental evolution of a drained lake at the Lousoi plateau (northern Peloponnese), for the last 10,000 years, through the study of a 7 m depth core. Analyses conducted on the core include grain size, TOC, TN, pH, EC, total carbonates (%), magnetic susceptibility measurements, XRF analysis, and radiocarbon dating. Our paleoenvironmental reconstruction was based on geochemical proxies' distribution in the core, combined with sediment physical and textural characteristics and later comparison between additional lacustrine archives from northern Peloponnese. From 10,900 to 7700 cal BP lacustrine, organic-rich deposits were recognized, reflecting increased lake water levels. Wet climatic conditions seem to have prevailed during this phase, interrupted by a dry pulse at 9400 cal BP. Transition to more shallow waters was marked at 8200 cal BP due to increased sediment deposition in the lake, with the environmental status shifting to a more oxygenated phase. Overall, wet conditions prevailed in this period and are in good agreement with regional records. In the Late Holocene period, the lake seems to have been highly affected by pedogenic processes, and thus, it was difficult to distinguish paleoclimatic/paleoenvironmental signals.

Keywords: XRF; polje; paleoenvironment; paleoclimate; eastern Mediterranean

Citation: Stamatis, D.; Emmanouilidis, A.; Masi, A.; Izdebski, A.; Avramidis, P. Holocene Hydroclimatic Changes in Northern Peloponnese (Greece) Inferred from the Multiproxy Record of Lake Lousoi. *Water* **2022**, *14*, 641. https://doi.org/10.3390/w14040641

Academic Editor: Hong Yang

Received: 6 December 2021
Accepted: 16 February 2022
Published: 18 February 2022

1. Introduction

The eastern Mediterranean region (Figure 1a) is shaped by high spatiotemporal variability of climate, produced by mid-latitude and subtropical atmospheric circulation systems [1,2]. The complex topography of the area further enhances this variability, with mountain ranges forming microclimates and distinct precipitation and temperature gradients. This climate complexity, combined with a long history of human occupation in the area, provides an ideal setting to track short- and long-term climatic and environmental fluctuations and even address how these changes affected early human societies.

The Peloponnese, in particular, is located in the transitional zone of large-scale atmospheric patterns and is characterized by an E–W precipitation gradient (Figure 1b). Climatic heterogeneity of the area is highlighted by studies conducted on lagoons [3,4], lakes [5,6], and speleothems [7]. Still, the chronological framework of most studies is limited to the Middle and Late Holocene; thus, data also reflecting the Early Holocene environmental and climatic status of the Peloponnese are lacking.

In this study, we present a new sedimentological archive from Lake Lousoi, located in the central part of Peloponnese (Figure 1b). The lake presents similar geomorphological and environmental characteristics to Stymphalia and Kaisari poljes [5,8], allowing a reliable and robust investigation and better evaluation of similar/opposing signals. Archaeological evidence in the area indicates that the region was inhabited at least from the Middle Neolithic (5700–5300 BCE) [9]. Our main aim is to track similar/opposing paleoclimatic

signals with previously studied sites of the Peloponnese and disentangle the general climatic regime of the area for the Middle-to-Late Holocene. Furthermore, additional studies from the broader Mediterranean region will be used, to evaluate and distinguish local events from regional ones.

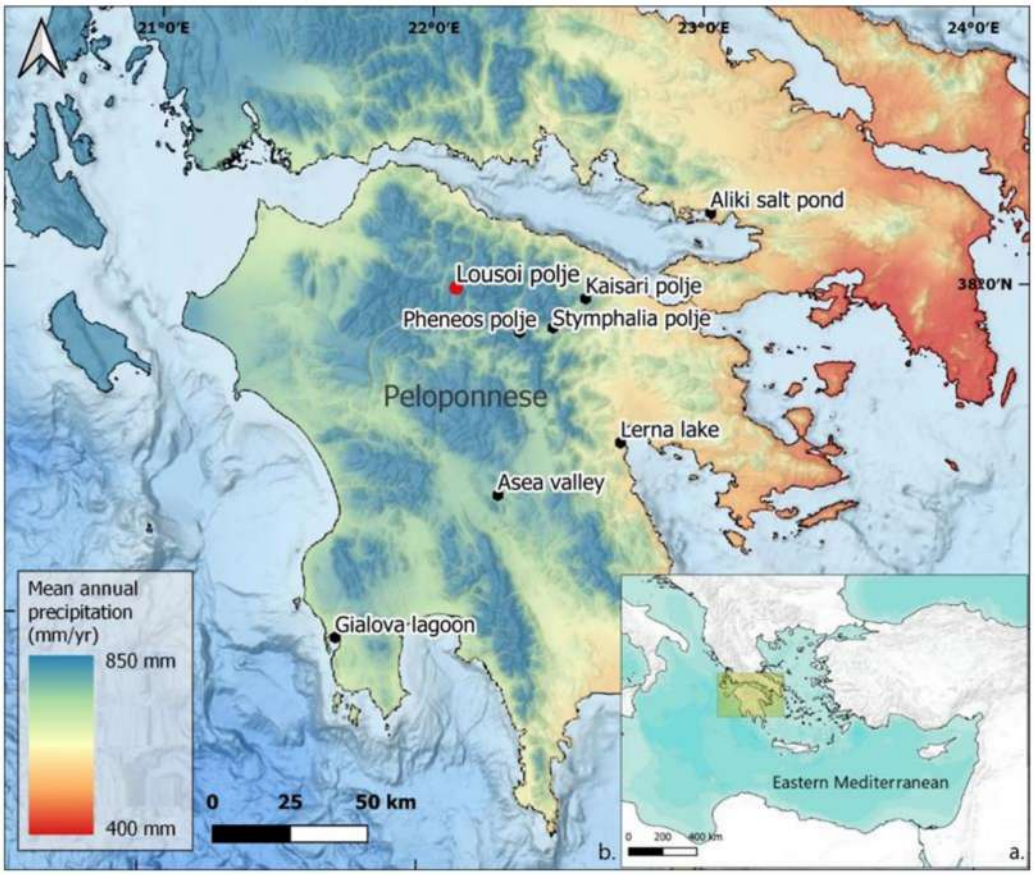

Figure 1. (**a**) Eastern Mediterranean map with the study area highlighted in yellow box; (**b**) map of Peloponnese, displaying the archives discussed in this study along with the mean annual precipitation of the region for the period 1970–2000 [10].

2. Study Area

2.1. Regional Setting

The catchment is located in the northern Peloponnese (Figure 1) and occupies an area of 78 km^2 (Figure 2). The area has steep topographic terrain, with altitudes ranging from 530 to 1629 m. Maximum altitude is observed on Mount Velia (1405 m), at the top of Prophet Elias in the northeastern part of the area (1629 m), at Psili Gouva, east of the village of Sigouni (1456 m) and Amolinitsa (1345 m) (Figure 2). Lake Lousoi is actually a polje set at an altitude of 940 m, with flat-surrounding terrain and a total surface area of 49 km^2 [11].

At the northern part of the study area, on the slopes of Mount Velia, the villages of Upper and Lower Lousoi are found (Figure 2) The watershed has a total surface of 28 km^2 with its northern limit constituted by the northwestern side of the mountain [11]. The catchment notably includes two sinkholes northwest of Lousiko, which drain the polje.

According to [12] the Peloponnese is classified as Csa (hot-summer Mediterranean climate) and receives, on average, between 400 and 850 mm of annual rainfall (Figure 1). Climatic data for the period 1975–1999 were taken from the meteorological stations of Lousika (1160 m), Kalavryta (731 m), Klitoria (750 m), and Lagovouni (880 m) of the Ministry of Rural Development and Food and Hellenic National Meteorological Service (HNMS). The wet period (October–March) in the region of Lousoi has an average precipitation of 114.31 mm/month (4.5 inches), while dry periods, from April until September, show an

average of 32.2 mm/month (1.26 inches). December is the wettest month, with 151.97 mm (5.98 inches) of precipitation, whereas August is the driest month, with 3.8 mm (0.14 inches). The average amount of total annual precipitation for the period 1975–1999 is 879.12 mm (34.61 inches).

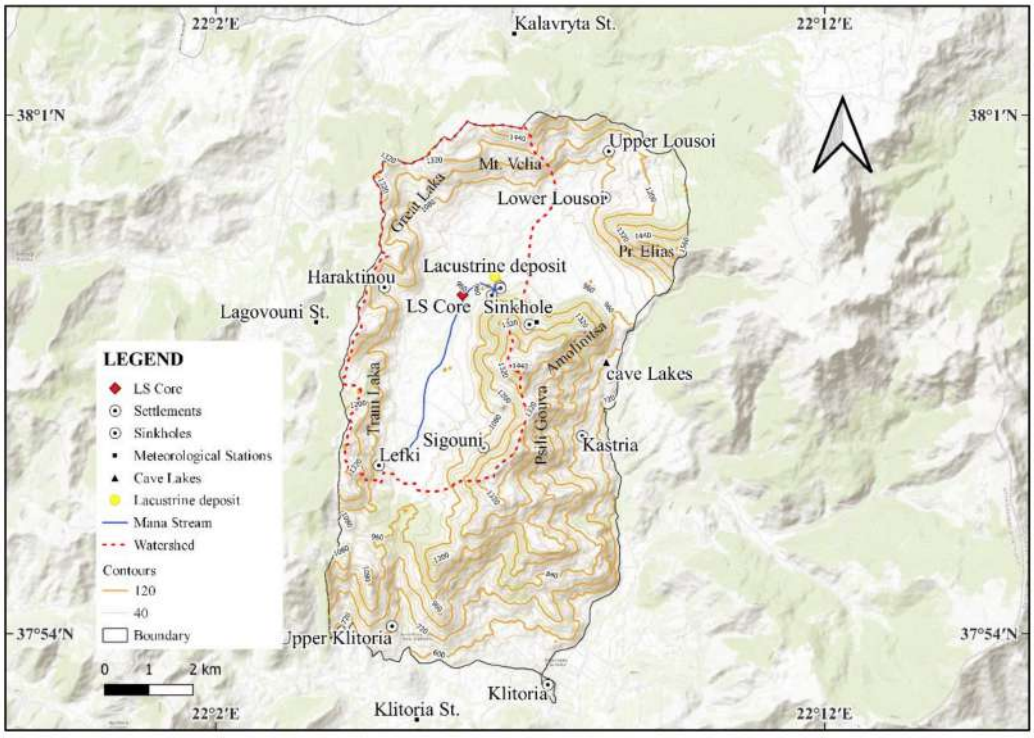

Figure 2. Geomorphological map of the study area presenting the main settlements and sinkholes, together with the core location, watershed, and drainage basin according to [11].

2.2. Geological Setting

The polje is dominated by Eocene flysch, Upper Cretaceous slabbed limestones, and Upper Jurassic siltstones and radiolarites (Figure 3). Upper Cretaceous undivided limestones and dolomites also appear in the northeastern part of the polje. The study area was formed mainly through the activity of two faults. The fault with a northwest/southeast direction in the center of the study area, which passes through the Cave of Lakes and the sinkholes, as well as a possible fault along the Mana stream, provides an explanation for the elongated shape of the valley [11].

The polje is drained by the Mana stream that is headed from the south to the north following the direction of the long axis of the valley, ending up in a pair of sinkholes, located at the center of the polje, at a height of 967 m. At the northern part of the sinkholes, a yellowish layer comprising lacustrine silty clay was found between alluvial deposits. The layer is believed to have been formed under a lake environment in the past and extended to a larger area around the polje [11]. Given the proximity of the sinkholes, the catchment must have been supplied with freshwater by the Mana stream that surpassed the drainage capacity of the sinkholes, thus forming a lake.

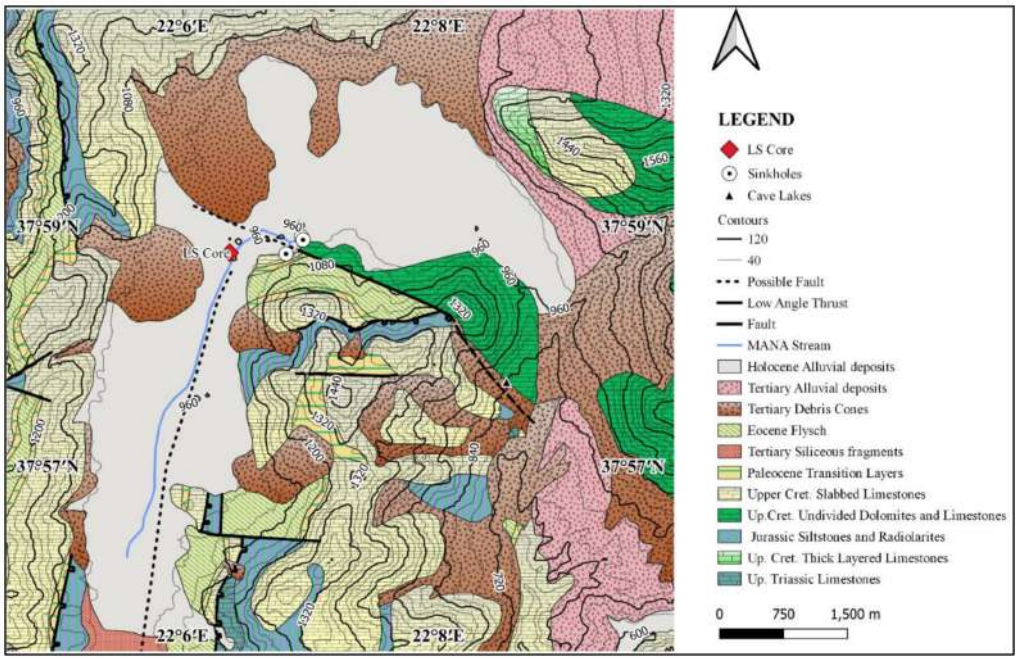

Figure 3. Geological map of the study area according to [13].

3. Materials and Methods

3.1. Coring Fieldwork

Fieldwork was conducted in early August 2020. The coring location was selected after inspection of the area and by assuming it represents the depocenter of the former lake. The exact location was recorded using a portable GPS device (37°58′25.25″ N, 22°6′11.97″ E). A 7 m long sediment core (LS core) was obtained using an Eijkelkamp percussion core sampler with sampling PVC closed tubes of 50 mm diameter and 1 m length. After coring, the sediment sequences were sealed with cling film and transported to the Department of Geology, University of Patras, Greece, where they were stored in cool rooms (4 °C).

3.2. Sedimentology

Standard sedimentological analysis was conducted on 77 samples from the sediment core (9 cm resolution) and analyzed grain size, carbonate content (%), magnetic susceptibility (MS), total organic carbon (TOC), total nitrogen (TN), pH, and electrical conductivity (EC).

The grain size of each sample was established using a Malvern Mastersizer, Hydro 2000, with the classification established according to [14]. Statistical grain-size parameters of the sediment were determined automatically through Gradistat V.4 software [15]. Total carbonates (%) were measured using a FOG II/Digital Hand-Held Calcimeter (BD Inventions [16,17]. MS measurements were obtained through a Bartington MS2E sensor, with 1 cm resolution throughout the sediment sequence. For the sediment color, first, high-resolution digital images were obtained using a Nikon DSLR camera and then processed through ImageJ software, to extract the RGB spectrum. TOC and TN were measured using 0.4 g of powdered sample and the TOC-VWS/WP Shimadzu Series Analyzer. For the pH measurement, 2 g of dry powdered sample (Ø < 2 mm) was mixed with 50 mL of deionized water [18]. The solution was left for 1 h for the nutrients to settle, after stirring. Then, measurements were taken by using an HQ40D digital two-channel multimeter. The solution was then filtered through a Whatman Medium filter paper and was followed by the measurement of electrical conductivity.

3.3. Elemental Variations and Radiocarbon Dating

Downcore elemental variations were measured by a Bruker XRF handheld scanner (S1 Titan/Tracer 5/CTX). A total of 140 measurements were pooled from the core segments with a 30 sec exposure time at 10–50 kV for the elements Al, Si, K, Ca, Ti, Mn, Fe, Rb, Sr, and Zr.

The chronological framework of the core was established through 4 ^{14}C radiocarbon dates conducted on bulk sediment. The analysis was performed at the Università Degli Campania Dipartimento di mathematica e fisica, CIRCE laboratory, in Napoli, Italy. Calibration of the radiocarbon dates was based on IntCal 20 [19]. Conventional and calibrated ages, as well as their exact depths, are presented in Table 1.

Table 1. List of radiocarbon dates conducted on core LS presented with depth (cm). Conventional dates were calibrated through IntCal20 calibration curve [19].

Lab ID	Depth (cm)	Sample Description	^{14}C Age (BP)	cal BP (2σ Ranges)
DSH9965	129	bulk sediment	1398 ± 29	1207–1381
DSH9964	298	bulk sediment	3999 ± 41	4258–4685
DSH9966	520	bulk sediment	7171 ± 43	7861–8163
DSH9543	672	bulk sediment	9294 ± 27	10301–10642

4. Results

4.1. Core Description and Stratigraphy

Based on the distribution of particle size, color, and sedimentary structures, four different sedimentary units were distinguished on the LS core. The presence of sand was low, ranging from 0.41 to 18%, whereas clay ranged from 25 to 63% and silt from 32 to 70% (Figure 4). The sedimentological/stratigraphic units recognized in the core are described in what follows.

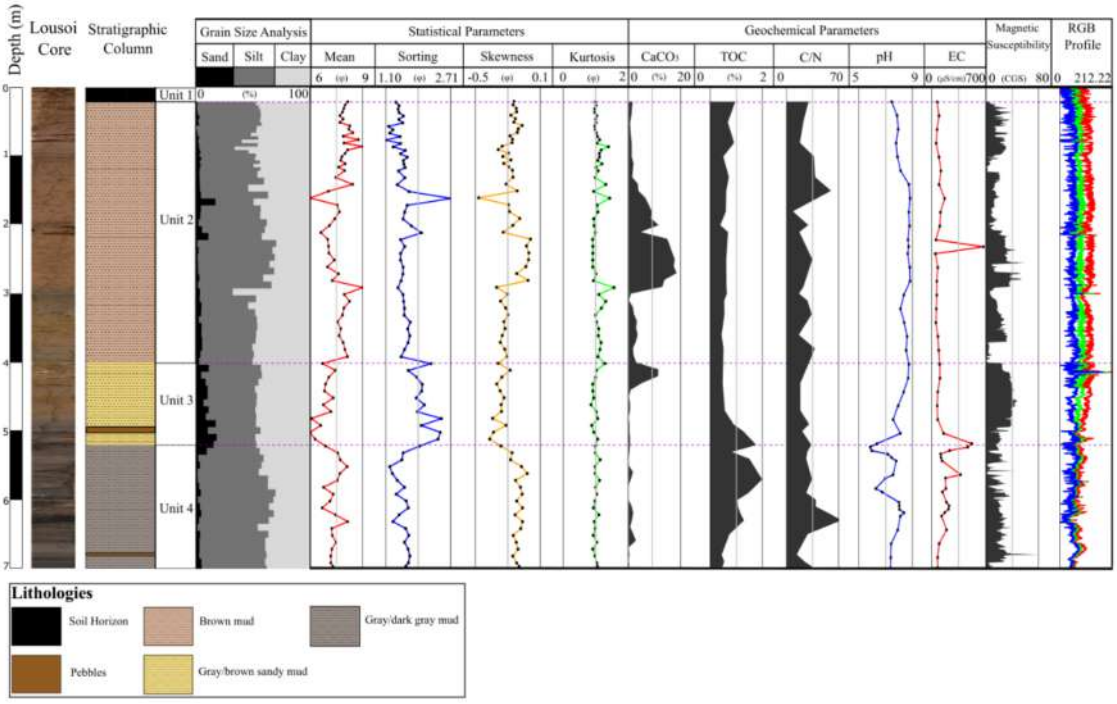

Figure 4. Log profile of core LS. From left to right, LS core photograph, stratigraphic column with the main units recognized, grain size distribution and statistical parameters, geochemical parameters ($CaCO_3$, TOC, C/N, pH, EC), magnetic susceptibility (MS) values, and RGB profile plot.

Unit 4 (5.20–7.00 m): This unit consists of poorly sorted gray-to-dark-gray mud. The sediment of this unit is very coarsely skewed to near-symmetrical, and the distribution is mainly mesokurtic with two measurements of leptokurtic material (5.45–5.40 m, 5.75–5.70 m). Pebbles were observed at 6.81–6.79 m.

Unit 3 (4.00–5.20 m): This unit consists mainly of poorly sorted, gray-to-brown sandy mud. Pebbles were observed at 5.00 m. The sediment is coarsely skewed to very coarsely skewed and primarily mesokurtic with two measurements (4.95–4.90 m, 4.65–4.60 m) of platykurtic material and one measurement (4.05–4.00 m) of leptokurtic material.

Unit 2 (0.20–4.00 m): This unit consists mainly of poorly sorted brown mud, with two intercalations of sandy mud at 1.62 and 2.12 m. The sediment of this unit is coarsely skewed, with a horizon of near-symmetrical material from 2.85 to 1.90.m The distribution ranges from mesokurtic to leptokurtic.

Unit 1 (0.00–0.20 m): This consists of the soil horizon that was not analyzed further, to avoid any erroneous measurements and interpretations.

Magnetic susceptibility is generally low throughout the core, with a mean value of 21.2 CGS (10^{-6} cm^3/g), except from zones of consistently higher values (6.90–5.90 m, 4.90–4.00 m, 2.90–2.80 m, 2.50–2.10 m, and 1.00–0.30 m) and an abrupt peak (6.80 m). The peak coincides with the appearance of coarser material (6.81–6.79 m) and a decrease in the C/N ratio (13.92) and TOC (0.44%). The carbonates (%) content is generally low at the lower part of the core and increases primarily at Unit 2. Increased values recognized from 4.20 to 4.10 m coincide with the increase in particle size and magnetic susceptibility. The same pattern is also observed from 2.82 to 2.55 m. Increased TOC ($\geq$1%) is observed at the lower parts of the LS core (6.35–5.00 m), whereas in the upper parts, values are <1%. The C/N ratio fluctuates throughout the core, presenting minimum values >10 and a maximum close to 60, thus supporting that TOC comes from terrestrial vascular plant material rather than protein-rich lake algae that would be reflected with molar C/N values between 4 and 10 [20]. One signal of probable autochthonous sedimentation is recognized from the C/N ratio from 1.85 to 1.80 m.

The pH and EC (electrical conductivity) in the LS core vary between the lower parts (7.00–5.00 m) and the upper parts (5.00–0.20 m) with mean pH values 7.32 and 8.34, respectively. Generally, the highest EC values were observed at the lower part of the core and coincide with increased TOC, whereas pH seems to reflect fluctuations in $CaCO_3$ content. Specifically, high EC values (5.30–5.15 m) were observed when pH was slightly acidic. Finally, the highest peaks in alkaline conditions (2.90–1.60 m) are associated with the highest concentrations in $CaCO_3$.

4.2. Radiocarbon Dating and Age–Depth Model

The age–depth model was constructed using the R package RBacon v.2.3 [21] and the IntCal20 calibration curve [19]. The top of the core was assigned at 2019 CE $\pm$ 10 years, which was the year of coring, and the bottom of the core sets at 10,900 cal BP (Figure 5). Radiocarbon dates seem to be in good accordance with each other, but the chronological control is relatively weak, given that the framework expands throughout the Holocene. Thus, our interpretation of climatic and environmental signals is limited to long-term oscillations rather than short-term events. The average sedimentation rate for the core is 0.06 cm/yr, which remained relatively stable for the entire sequence.

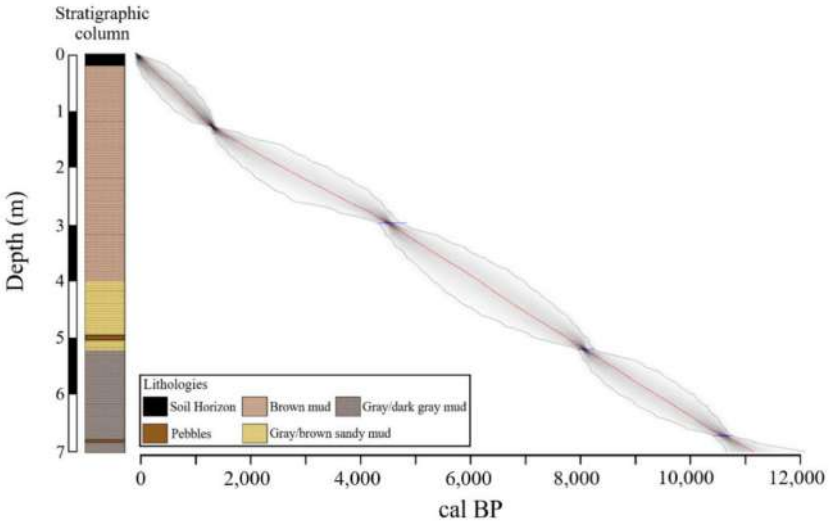

Figure 5. Age–depth model for LS core, constructed using the R package RBacon [21]. The blue tie bars indicate the ^{14}C age distributions (Table 1). The grayscale of the line graph reflects the likelihood, and the red dotted line follows the mean ages.

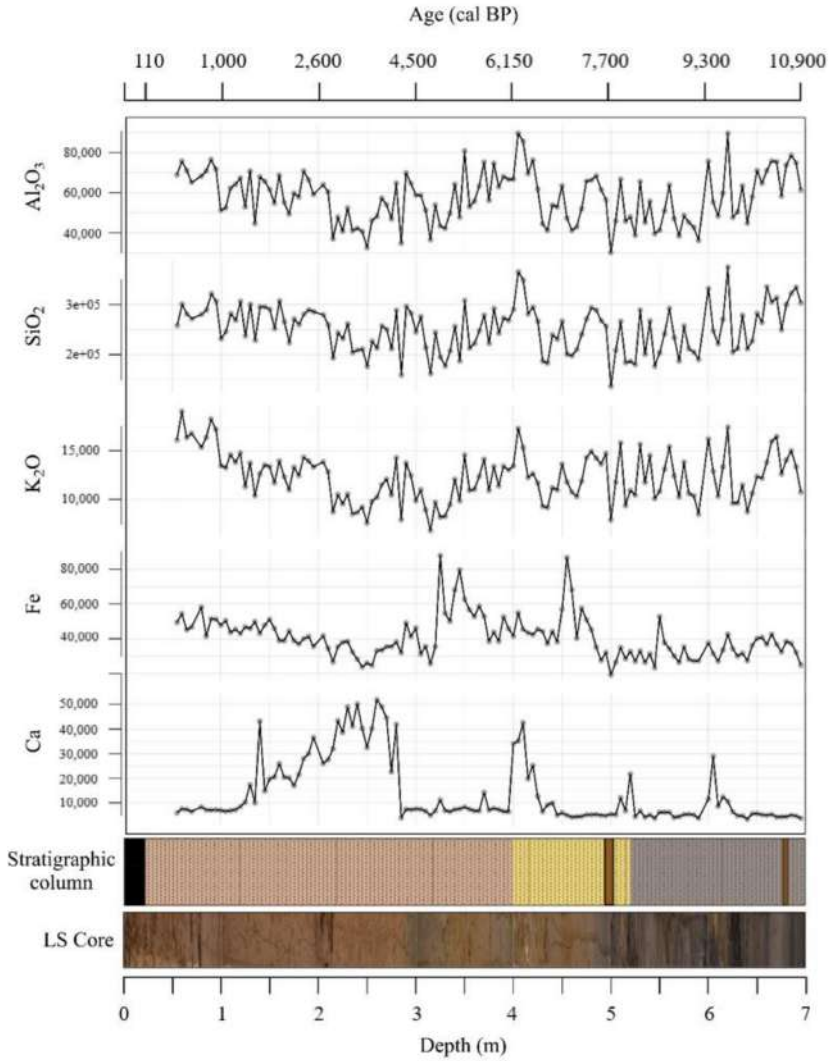

Figure 6. Geochemical proxies' distribution against depth (m) and age (cal BP), with the stratigraphic column and LS core presented at the bottom. Concentration of each element is presented in counts (cps).

4.3. Distribution of Geochemical Proxies

The downcore elemental profiles from the LS core present large variations that are clearly linked with changes in sediment composition and properties. Elements such as Si, Al, and K exhibit a similar distribution in the core and are mostly transported in the system during periods of increased clastic inwash (Figure 6). Si seems to be mostly of detrital rather than biogenic origin since Si distribution in the core is similar to the other detrital-originated elements (Al and K) (Figure 6). No distinct pattern can be observed for Si, K, and Al distributions, apart from some periods at 7.00

6.20 m, 4.20–4.70 m, 3.00–4.00 m, and 1.00–1.80 m (Figure 6). Fe, which is highly influenced by redox conditions prevailing in the system, presents low concentrations for the most part of the core, except from some increased values recorded at 4.30–4.60 m and 3.00–3.50 m (Figure 6). The Ca profile is clearly correlated with the total carbonates (%) content (Figure 4), with distinct increases recorded at Units 2 and 3 (Figure 6).

5. Discussion

Lacustrine records studied so far in northern Peloponnese (Stymphalia, Kesari, Pheneos, and Asea) represent shallow water bodies that have experienced long periods of desiccation and are highly influenced by climatic/environmental forcing, anthropogenic activity, and pedogenic processes [5,8,22]. To summarize the geochemical composition from the prior mentioned sedimentary sequences, previous studies have used principal component analysis, with PC1 explaining the inflow of carbonate-rich clastic material during periods of increased weathering in the catchment, whereas PC2 explains the enhanced carbonate precipitation during dry–warm conditions [8]. We applied the same method here for these sites, but for Lake Lousoi, the resolution of our geochemical data did not permit a robust analysis; thus, we interpreted each geochemical proxy separately (Figure 7).

5.1. Early Holocene (11,800–8200 cal BP)

From 10,900 to 8200 cal BP (7.00–5.20 m), the Lake Lousoi sediment sequence presents a typical organic-rich lake deposit, interrupted by an intermediate thin layer of pebbles at 10,800 cal BP (Figure 4). TOC and pH measurements for this period (Figure 4) indicate a relatively alkaline environment with sufficient water levels to permit organic matter preservation. Detrital originated elements such as Si, Al and K present increased values, with a minor decrease at 9400 that is followed by an increase in Ca, probably due to a dry–warm pulse and increase in carbonate ions precipitation in the system (Figures 6 and 7). A similar signal of dry conditions but with a longer duration was recorded for the Balkans from 9900 to 8900 [23].

The Pheneos sedimentary sequence, which is the only record from the area expanding in the same timeframe as Lake Lousoi, exhibits overall humid conditions until 8900 cal BP, with two short dry phases recorded at 10,300 and 10,000 cal BP (Figure 7). On a more regional scale, the Early Holocene period is marked with $\delta^{18}O$ depletion in lakes and speleothems [24,25], thus indicating relatively warm and wet climatic conditions.

5.2. Middle Holocene (8200–4200 cal BP)

At the start of the Middle Holocene, the sediment record from Lake Lousoi gradually transits to a gray/brown coarser material (Figure 4). This transition is also accompanied by a decrease in TOC (Figure 4), indicating that the lake must have reached a more oxygenated phase, where the water level was considerably lower and fluctuated during seasons. In addition, a slight increase in Ca content at 8200 cal BP indicates increased evaporation and may be attributed to the 8.2 events that produced long-term cold–dry trends [26] (Figure 6). From this point on, Ca content seems to change drastically in terms of total counts and is also highly correlated with detrital elements' distribution. This points to a common source of these elements, meaning that Ca was mostly transported in the system from an allochthonous source rather than biogenic/chemical processes. Fe concentration also

presents increased values from 7400 to 4800 cal BP and coincides with increased values of MS (Figure 4), which reflect increased detrital inflow in the system.

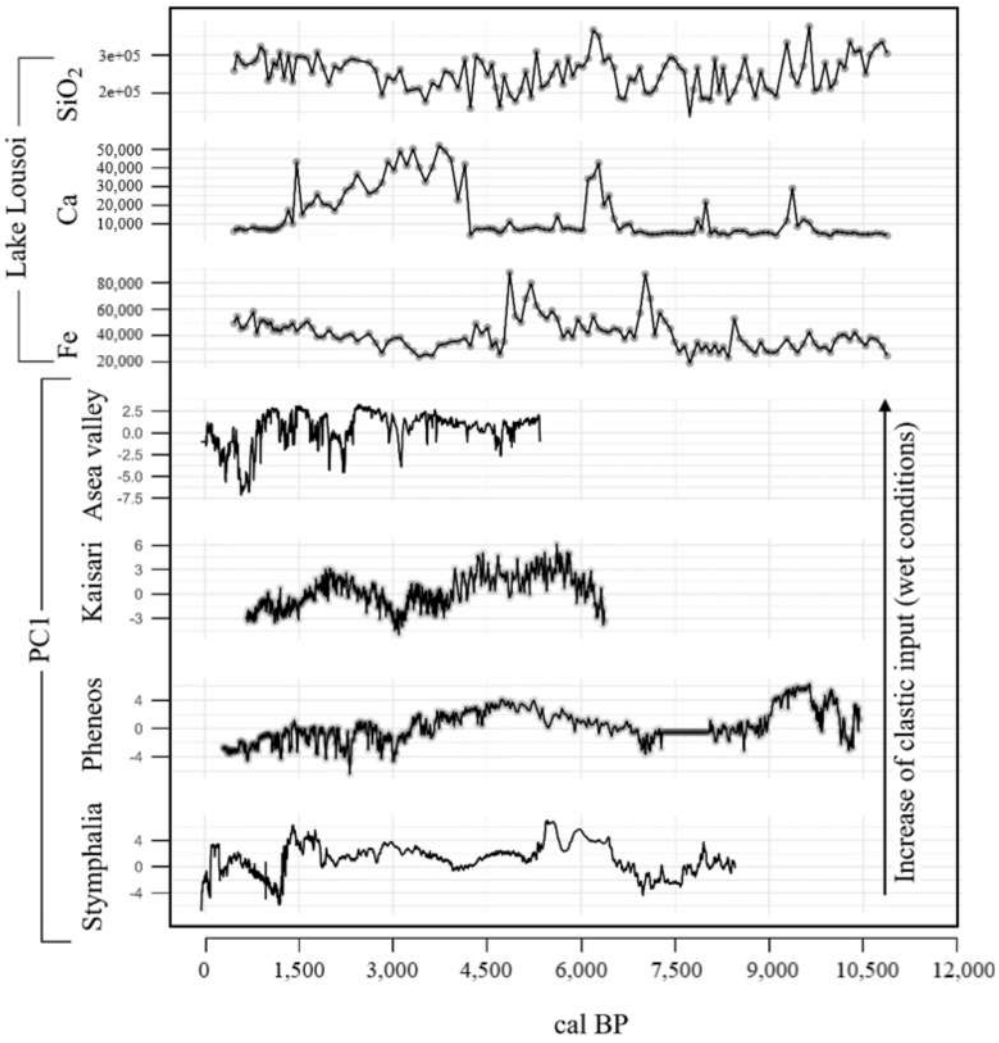

Figure 7. Comparison of the geochemical proxies from Lake Lousoi with the PC1 distributions from Asea valley and Lakes Kaisari, Pheneos, and Stymphalia.

Overall, humid conditions were reported in the other lacustrine records of the Peloponnese during the Middle Holocene (Figure 7). In Lake Stymphalia, which presents similar geomorphological characteristics like Lake Lousoi, a dry period was recorded from 7600 to 6700 cal BP, followed by a transition to more humid conditions until 4500 cal BP [5] (Figure 7). Same signals with increased detrital inflow were recorded for Lakes Lousoi, Pheneos, and Kaisari, especially from 6700 to 5800 cal BP, where the highest concentration of detrital elements and MS are recorded (Figures 4 and 6). At Lake Pheneos, south of Lake Lousoi, the system seems to be a permanent water body from 5000 to 3600 cal BP, due to wet climatic conditions and perpetual supply of fresh water [8]. More to the south, the Asea valley's record presents stable conditions and lack of lake sediments from 5000 to 3400 cal BP, with some minor dry trends recorded at 4900 and 4700 cal BP [22].

Regional climatic records from the Balkans in general display stable climatic conditions [27] for the Middle Holocene, with high lake levels recorded at Lake Prespa [28], Lake Dojran [29] and Lake Van [30]. Opposing trends of aridification are displayed in the eastern Mediterranean at Eski Acigöl [31] and Lake Pergusa [32]. In Lake Ohrid, a shift in the erosional processes was recorded after the cooling event of 8.2, pointing to a vegetation-controlled landscape erosion rather than a rainfall controlled [33]. Similarly, wet

climatic trends were recorded from 5000 to 3500 cal BP in the northern Aegean [34] and Lake Lerna [6].

5.3. Late Holocene (4200 cal BP–Present)

The onset of the Late Holocene at 4200 cal BP is marked with an abrupt increase in Ca concentration until 1500 cal BP. Since no macroshell remains were identified in the sediment core, we assume that calcium carbonate in the system is mostly derived as nodules, indicating the formation of pedogenic soil and post-depositional alteration of the sediment. C/N ratio also indicates an allochthonous source of organic material during this period, with decreased TOC values through the sequence. Since the sediment core was retrieved from the depocenter of the lake, at least according to the geomorphological features of the area, we assume that after 4200 cal BP, the lake Lousoi must have reached a state close to its present, with episodes of seasonal flooding being the main supply of fresh water in the area. Whether the 4.2 cold–dry event [35] was the main driving factor of Lake Lousoi transition at this state is hard to tell due to our age–depth model's uncertainty and also due to the extensive anthropogenic activity in the area that may also contributed to drainage activities of the lake. All in all, the last 4000 years of Lake Lousoi may be highly affected by pedogenic processes, and thus, it was difficult to distinguish paleoclimatic and paleoenvironmental signals.

6. Conclusions

The lacustrine records of northern Peloponnese reveal a complex environmental history, highly affected by past climatic status and anthropogenic activity. In this study, we used a multiproxy approach on a 7 m long sediment core from Lake Lousoi, to identify similar/opposing trends between local and regional archives. Our data indicate that, for the last 10,900 years, Lake Lousoi experienced significant changes that led to final desiccation at around 4200 cal BP. During the Early Holocene, typical lacustrine organic-rich deposits indicated a lake system with enough water supply to maintain a permanent water body. Wet climatic conditions were also recognized in the same period and reflected by enhanced weathering in the catchment and inflow of detrital-originated elements. A transitional stage at 8200 cal BP coincided with the hemispheric 8.2 cold–dry event, resulting in shallower lake waters. After this, the study area seemed to be still supplied with fresh water but reached a more oxygenated phase, as indicated by the TOC and pH measurements. Overall, wet climatic conditions were recorded from 7700 to 4600 cal BP and are in good agreement with those of Lakes Kaisari and Stymphalia. At 4200 cal BP, an abrupt increase in Ca was recorded, and Lake Lousoi shifted to a state close to its present, where water level fluctuates according to seasonal flooding.

Author Contributions: Conceptualization, P.A.; methodology, P.A., A.E. and D.S; software, A.E. and D.S.; validation, P.A., A.E., A.I. and A.M.; investigation, D.S.; resources, P.A., A.I. and A.M.; data curation, D.S.; writing—original draft preparation, D.S.; writing—review and editing, A.E., P.A., A.I. and A.M.; visualization, D.S. and A.E.; supervision, P.A.; project administration, P.A.; funding acquisition, P.A. All authors have read and agreed to the published version of the manuscript.

Funding: This study was funded by the Max Planck Institute for the Science of Human History, project title "Environmental history of the Byzantine and Ottoman Peloponnese".

Institutional Review Board Statement: Not applicable.

Informed Consent Statement: Not applicable.

Data Availability Statement: Data are available on request from the corresponding author.

Acknowledgments: We would like to thank Giannis Prevedouros, Dimitris Bassukas, and Dionysis Christodoulopoulos for the help they provided during the coring campaign of this project.

Conflicts of Interest: The authors declare no conflict of interest.

References

1. Ulbrich, I.M.; Canagaratna, M.R.; Cubison, M.J.; Zhang, Q.; Ng, N.L.; Aiken, A.C.; Jimenez, J.L. Three-Dimensional Factorization of Size-Resolved Organic Aerosol Mass Spectra from Mexico City. *Atmos. Meas. Tech.* **2012**, *5*, 195–224. [CrossRef]
2. Giorgi, F. Climate Change Hot-Spots. *Geophys. Res. Lett.* **2006**, *33*, L08707. [CrossRef]
3. Emmanouilidis, A.; Katrantsiotis, C.; Norström, E.; Risberg, J.; Kylander, M.; Sheik, T.A.; Iliopoulos, G.; Avramidis, P. Middle to late Holocene palaeoenvironmental study of Gialova Lagoon, SW Peloponnese, Greece. *Quat. Int.* **2018**, *476*, 46–62. [CrossRef]
4. Katrantsiotis, C.; Kylander, M.E.; Smittenberg, R.; Yamoah, K.K.A.; Hättestrand, M.; Avramidis, P.; Strandberg, N.A.; Norström, E. Eastern Mediterranean Hydroclimate Reconstruction over the Last 3600 Years Based on Sedimentary N-Alkanes, Their Carbon and Hydrogen Isotope Composition and XRF Data from the Gialova Lagoon, SW Greece. *Quat. Sci. Rev.* **2018**, *194*, 77–93. [CrossRef]
5. Seguin, J.; Bintliff, J.L.; Grootes, P.M.; Bauersachs, T.; Dörfler, W.; Heymann, C.; Manning, S.W.; Müller, S.; Nadeau, M.J.; Nelle, O.; et al. 2500 Years of Anthropogenic and Climatic Landscape Transformation in the Stymphalia Polje, Greece. *Quat. Sci. Rev.* **2019**, *213*, 133–154. [CrossRef]
6. Katrantsiotis, C.; Norström, E.; Smittenberg, R.H.; Finne, M.; Weiberg, E.; Hättestrand, M.; Avramidis, P.; Wastegård, S. Climate Changes in the Eastern Mediterranean over the Last 5000 years and Their Links to the High-Latitude Atmospheric Patterns and Asian Monsoons. *Glob. Planet. Chang.* **2019**, *175*, 36–51. [CrossRef]
7. Finné, M.; Bar-Matthews, M.; Holmgren, K.; Sundqvist, H.S.; Liakopoulos, I.; Zhang, Q. Speleothem evidence for late Holocene climate variability and floods in Southern Greece. *Quat. Res.* **2014**, *81*, 213–227. [CrossRef]
8. Seguin, J.; Avramidis, P.; Haug, A.; Kessler, T.; Schimmelmann, A.; Unkel, I. Reconstruction of Palaeoenvironmental Variability Based on an Inter-Comparison of Four Lacustrine Archives on the Peloponnese (Greece) for the Last 5000 Years. *E G Quat. Sci. J.* **2020**, *69*, 165–186. [CrossRef]
9. Facorellis, Y.; Maniatis, Y. 14 C dating of samples from the cave of Lakes at Kastria of Kalavrita. In *The Cave of Lakes at Kastria of Kalavryta. A Prehistoric Site in the Highlands of Peloponnese*; Sampson, A., Ed.; Society of Peloponnesian Studies: Athens, Greece, 1997; pp. 527–531.
10. Fick, S.E.; Hijmans, R.J. WorldClim 2: New 1-Km Spatial Resolution Climate Surfaces for Global Land Areas. *Int. J. Climatol.* **2017**, *37*, 4302–4315. [CrossRef]
11. Koutsi, J.R. *The Role of Epikarst in the Assessment and Mapping of the Vulnerability of Karstic Formations through the Use of a New European Method*; 2007. (In Greek)
12. Köppen, W.; Geiger, R. *Handbuch Der Klimatologie: Das Geographische System Der Klimate*; Gebrüder Borntraeger: Berlin, Germany, 1936; Volume 35.
13. Institute of Geology and Mineral Exploration. *Daphnie Sheet, 1:50000, Athens, Greece*; Institute of Geology and Mineral Exploration: Thessaloniki, Greece, 1978.
14. Folk, R.L.; Andrews, P.B.; Lewis, D.W. Detrital Sedimentary Rock Classification and Nomenclature for Use in New Zealand. *N. Z. J. Geol. Geophys.* **1970**, *13*, 937–968. [CrossRef]
15. Blott, S.J.; Pye, K. Gradistat: A Grain Size Distribution and Statistics Package for the Analysis of Unconsolidated Sediments. *Earth Surf. Processes Landf.* **2001**, *26*, 1237–1248. [CrossRef]
16. Müller, G.; Gastner, M. The "Karbonat-Bombe", a Simple Device for the Determination of Carbonate Content in Sediment, Soils, and Other Materials. *Neues Jahrb. Für Mineral.-Mon.* **1971**, *10*, 466–469.
17. Jones, G.A.; Kaiteris, P. A Vacuum-Gasometric Technique for Rapid and Precise Analysis of Calcium Carbonate in Sediments and Soils. *J. Sediment. Petrol.* **1983**, *53*, 655–660. [CrossRef]
18. Hoffmann, G. *Methodenbuch Band 1: Die Untersuchung von Böden. Verband Deutscher Landwirtschaftlicher Untersuchungs und Forschungsanstalten*; VDLUFA-Verlag: Darmstadt, Germany, 1991; ISBN 978-3-941273-25-2.
19. Reimer, P.J.; Austin, W.E.N.; Bard, E.; Bayliss, A.; Blackwell, P.G.; Bronk Ramsey, C.; Butzin, M.; Cheng, H.; Edwards, R.L.; Friedrich, M.; et al. The IntCal20 Northern Hemisphere Radiocarbon Age Calibration Curve (0-55 Cal KBP). *Radiocarbon* **2020**, *62*, 725–757. [CrossRef]
20. Meyers, P.A. Applications of Organic Geochemistry to Paleolimnological Reconstructions: A Summary of Examples from the Laurentian Great Lakes. *Org. Geochem.* **2003**, *34*, 261–289. [CrossRef]
21. Blaauw, M.; Christeny, J.A. Flexible Paleoclimate Age-Depth Models Using an Autoregressive Gamma Process. *Bayesian Anal.* **2011**, *6*, 457–474. [CrossRef]
22. Unkel, I.; Schimmelmann, A.; Shrin, C.; Forsén, J.; Heymann, C.; Brückner, H. The Environmental History of the Last 6500 Years in the Asea Valley (Peloponnese, Greece) and Its Linkage to the Local Archaeological Record. *Z. Für Geomorphol.* **2014**, *58*, 89–107. [CrossRef]
23. Finné, M.; Woodbridge, J.; Labuhn, I.; Roberts, C.N. Holocene Hydro-Climatic Variability in the Mediterranean: A Synthetic Multi-Proxy Reconstruction. *Holocene* **2019**, *29*, 847–863. [CrossRef]
24. Roberts, N.; Jones, M.D.; Benkaddour, A.; Eastwood, W.J.; Filippi, M.L.; Frogley, M.R.; Lamb, H.F.; Leng, M.J.; Reed, J.M.; Stein, M.; et al. Stable Isotope Records of Late Quaternary Climate and Hydrology from Mediterranean Lakes: The ISOMED Synthesis. *Quat. Sci. Rev.* **2008**, *27*, 2426–2441. [CrossRef]
25. Bar-Matthews, M.; Ayalon, A.; Kaufman, A. Late Quaternary Paleoclimate in the Eastern Mediterranean Region from Stable Isotope Analysis of Speleothems at Soreq Cave, Israel. *Quat. Res.* **1997**, *47*, 155–168. [CrossRef]

26. Rohling, E.J.; Pä, H. Centennial-Scale Climate Cooling with a Sudden Cold Event around 8,200 Years Ago. *Nature* **2005**, *434*, 975–979. [CrossRef] [PubMed]
27. Aufgebauer, A. Climate Change in the Balkan Region during the Late Glacial and the Holocene Recorded in the Lake Prespa Sediment Sequence. *Quat. Int.* **2012**, *279–280*, 28. [CrossRef]
28. Leng, M.J.; Wagner, B.; Boehm, A.; Panagiotopoulos, K.; Vane, C.H.; Snelling, A.; Haidon, C.; Woodley, E.; Vogel, H.; Zanchetta, G.; et al. Understanding Past Climatic and Hydrological Variability in the Mediterranean from Lake Prespa Sediment Isotope and Geochemical Record over the Last Glacial Cycle. *Quat. Sci. Rev.* **2013**, *66*, 123–136. [CrossRef]
29. Francke, A.; Wagner, B.; Leng, M.J.; Rethemeyer, J. A Late Glacial to Holocene Record of Environmental Change from Lake Dojran (Macedonia, Greece). *Clim. Past* **2013**, *9*, 481–498. [CrossRef]
30. Litt, T.; Krastel, S.; Sturm, M.; Kipfer, R.; Örcen, S.; Heumann, G.; Franz, S.O.; Ülgen, U.B.; Niessen, F. "PALEOVAN", International Continental Scientific Drilling Program (ICDP): Site Survey Results and Perspectives. *Quat. Sci. Rev.* **2009**, *28*, 1555–1567. [CrossRef]
31. Roberts, N.; Jones, M. Towards a Regional Synthesis of Mediterranean Climatic Change Using Lake Stable Isotope Records. *PAGES News* **2002**, *10*, 13–15. [CrossRef]
32. Sadori, L.; Narcisi, B. The Postglacial Record of Environmental History from Lago Di Pergusa, Sicily. *Holocene* **2001**, *11*, 655–671. [CrossRef]
33. Francke, A.; Dosseto, A.; Panagiotopoulos, K.; Leicher, N.; Lacey, J.H.; Kyrikou, S.; Wagner, B.; Zanchetta, G.; Kouli, K.; Leng, M.J. Sediment Residence Time Reveals Holocene Shift from Climatic to Vegetation Control on Catchment Erosion in the Balkans. *Glob. Planet. Chang.* **2019**, *177*, 186–200. [CrossRef]
34. Psomiadis, D.; Dotsika, E.; Albanakis, K.; Ghaleb, B.; Hillaire-Marcel, C. Speleothem Record of Climatic Changes in the Northern Aegean Region (Greece) from the Bronze Age to the Collapse of the Roman Empire. *Palaeogeogr. Palaeoclimatol. Palaeoecol.* **2018**, *489*, 272–283. [CrossRef]
35. Staubwasser, M.; Weiss, H. Holocene Climate and Cultural Evolution in Late Prehistoric-Early Historic West Asia. *Quat. Res.* **2006**, *66*, 372–387. [CrossRef]